Bull Volcanol (2006) 68: 407–419
DOI 10.1007/s00445-005-0015-8

RESEARCH ARTICLE

Ian S. E. Carmichael · Holli M. Frey · Rebecca A. Lange · Chris M. Hall

The Pleistocene cinder cones surrounding Volcán Colima, Mexico re-visited: eruption ages and volumes, oxidation states, and sulfur content

Received: 16 August 2004 / Accepted: 18 May 2005 / Published online: 28 January 2006

Abstract Located at the volcanic front in the western Mexican arc, in the Colima Rift, is the active Volcán Colima, which lies on the southern end of the massive (~450 km^3) Colima-Nevado volcanic complex. Along the margins of this andesitic volcanic complex, is a group of 11 scoria cones and associated lavas, which have been dated by the $^{40}Ar/^{39}Ar$ method. Nine scoria cones erupted ~1.3 km^3 of alkaline magma (basanite, leucite-basanite, minette) between 450 and 60 ka, with >99% between 240 and 60 ka. Two additional cones (both the oldest and calc-alkaline) erupted <0.003 km^3 of basalt (0.5 Ma) and <0.003 km^3 of basaltic andesite (1.2 Ma), respectively. Cone and lava volumes were estimated with the aid of digital elevation models (DEMs). The eruption rate for these scoria cones and their associated lavas over the last 1.2 Myr is ~1.2 km^3/Myr, which is more than 400 times smaller than that from the andesitic Colima-Nevado edifice. In addition to these alkaline Colima cones, two other potassic basalts erupted at the volcanic front, but ~200 km to the ESE (near the historically active Volcán Jorullo), and were dated at 1.06 and 0.10 Ma. These potassic suites reflect the tendency in the west-central Mexican arc for magmas close to the volcanic front to be enriched in K_2O relative to those farther from the trench.

Ferric-ferrous analyses on pristine samples from the alkaline cones adjacent to V. Colima and V. Jorullo indicate that their oxygen fugacities relative to the nickel-nickel oxide buffer are significantly higher (ΔNN0=2–4) than those for the calc-alkaline magma types (0–1.5). These ΔNNO values correlate positively with Ba concentrations and likely reflect the influence of a slab-derived fluid. As a result of the high oxidation states, the solubility of sulfur in these potassic magmas is enhanced. Indeed the sulfur content of both the whole rock and the apatite phenocrysts (and in olivine melt inclusions reported in the literature) suggest that part of their pre-eruptive sulfur gas (SO_2) concentrations could have been discharged to the atmosphere in amounts comparable to the 1982 eruption of El Chichón, although over a prolonged period spanning thousands of years (not per eruption).

Electronic Supplementary Material Supplementary material is available for this article at http://dx.10.1007/s00445-005-0015-8

Editorial responsibility: J. Donnelly-Nolan

I. S. E. Carmichael (✉)
Department of Earth and Planetary Science, University of California,
307 McCone Hall, Berkeley, CA 94720
e-mail: ian@eps.berkeley.edu
Tel.: 510-642-2577
Fax: 510-643-9980

H. M. Frey · R. A. Lange · C. M. Hall
Department of Geological Sciences, University of Michigan,
2534 C.C. Little Building, Ann Arbor, MI 48109

Introduction

The west-central Mexican volcanic arc is related to subduction of the Rivera and Cocos plates beneath the North American Plate along the Middle America Trench (Fig. 1). The tectonics of the upper plate are dominated by three intersecting rift systems: (1) the N–W trending Tepic-Zacoalco Rift, (2) the N–S trending Colima Rift, and (3) the E–W Chapala Rift that contains Lake Chapala (Fig. 1). Within the Colima Rift is a massive, southward-younging chain of three andesitic, composite volcanoes (Figs. 1 and 2). The active Volcán Colima is found at the southernmost end of this complex, whereas 5 km to the north is the larger Pleistocene volcano, Nevado de Colima (Fig. 2). In combination, the Colima-Nevado volcanic edifice has a volume of ~450 km^3, and the surrounding volcaniclastic apron has a comparable volume (Luhr and Carmichael 1980). Approximately 15 km farther north is the eroded andesitic/dacitic volcanic center of Cerro El Cántaro.

Along the northern margin of the Colima-Nevado edifice is a group of 10 cinder cones (Fig. 2); an 11th cone is ~10 km N off the map in Fig. 2. Nine of the 11 scoria cones are made of alkaline rock types (basanite, leucite-basanite, and minette), whereas two are calc-alkaline scoria

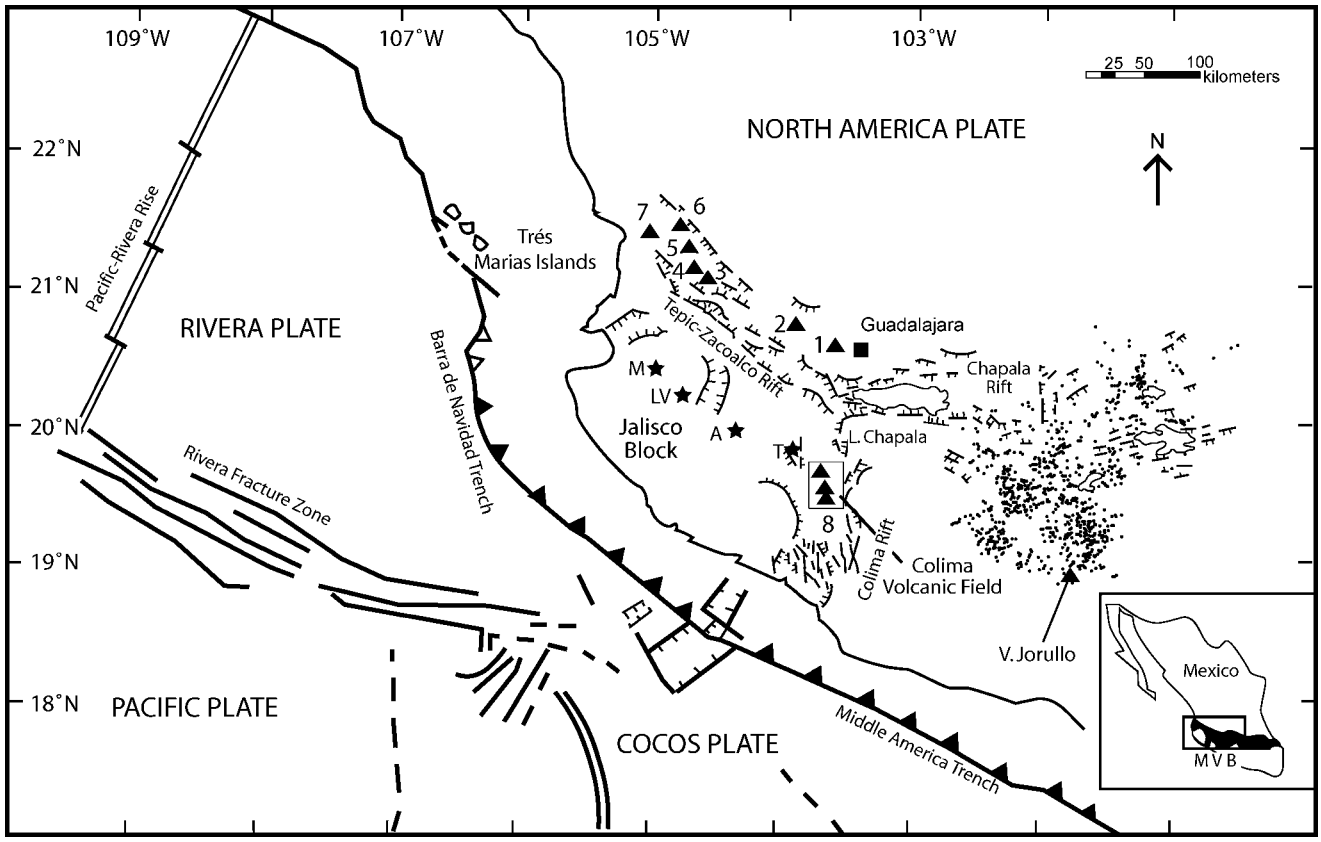

Fig. 1 General tectonic and geologic map of western Mexico, modified from Delgado-Granados (1993). *Numbered triangles* in the Tepic-Zacoalco and Colima grabens refer to central volcanoes of the Mexican Volcanic Belt: (*1*) Sierra La Primavera, (*2*) V. Tequila, (*3*) V. Ceboruco, (*4*) V. Tepetiltic, (*5*) V. Sanganguey, (*6*) V. Las Navajas, (*7*) V. San Juan, and (*8*) V. Colima-Nevado. The Michoacán-Guanajuato volcanic field (MGVF) consists of numerous vents, represented by *solid dots*. V. Jorullo is a cinder cone at the volcanic front within the MGVF. Tectonic elements are from DeMets and Stein (1990) and Johnson and Harris (1990). The letters *M*, *LV*, *A*, and *T* refer to the towns of Mascota, Los Volcanes, Ayutla and Tapalpa, respectively

cones of basaltic andesite and basalt, respectively (Luhr and Carmichael 1981). Collectively, the alkaline cones and their associated lavas stand in remarkable compositional and mineralogical contrast to the plagioclase-abundant lavas of the andesitic stratovolcanoes.

Alkaline, phlogopite-bearing cinder cones and associated lavas are also found (near the towns of Mascota, Los Volcanes, Ayutla, and Tapalpa) within interior extensional grabens of the Jalisco Block, which is bounded by the Tepic-Zacoalco Rift, the Colima Rift and the Middle America Trench (Fig. 1; Carmichael et al. 1996; Wallace and Carmichael 1992a; Righter and Rosas-Elguera 2001). In addition to this clear association of alkaline volcanic rocks with grabens of the Jalisco Block, potassic magmas also erupted ~200 km to the ESE along the volcanic front. Here, close to the historically active cone of Jorullo (Fig. 1; Luhr and Carmichael 1985), a trachybasalt with hornblende ±phlogopite phenocrysts erupted at Cerro La Pilita.

When the 11 scoria cones adjacent to the andesitic stratovolcanoes of Volcán Colima and Nevado de Colima were first mapped and described more than 20 years ago (Luhr and Carmichael 1981), there were no radiometric dates for any of the scoria or associated lavas. Nor were there any radiometric dates for the andesite volcanoes themselves. Subsequently, four K-Ar ages published by Allan (1986) show that the Cantaro volcanic complex was active at ~1–1.5 Ma, whereas seven K-Ar ages reported by Robin et al. (1987) indicate that Nevado de Colima was active between ~0.53 and ~0.08 Ma. These dates lead to the question: Were these 11 cinder cones erupted over a relatively broad time interval, spanning the last 1 Myr and contemporaneous with the entire history of andesitic volcanism in the Colima Rift? Or, alternatively, were the 11 cones erupted over a relatively narrow and recent interval (e.g., over the last 40 kyr) as initially suggested by Luhr and Carmichael (1981)? To address these issues, we used the laser-heated $^{40}Ar/^{39}Ar$ technique to date 12 samples from these 11 cones and their associated lavas. We combine these dates with estimates of erupted volumes using digital elevation models (DEMs) and ortho airphotos so that a more precise eruption rate for these mantle-derived, potassic magmas can be obtained.

Other questions relate to the oxidation state and sulfur concentrations of these magmas, and whether there was a significant release of SO_2 during their eruption. Although the cones are small in volume, some have associated flows that, in aggregate, may rival the erupted volume (~0.4 km^3) of the sulfur-rich and oxidized magma from El

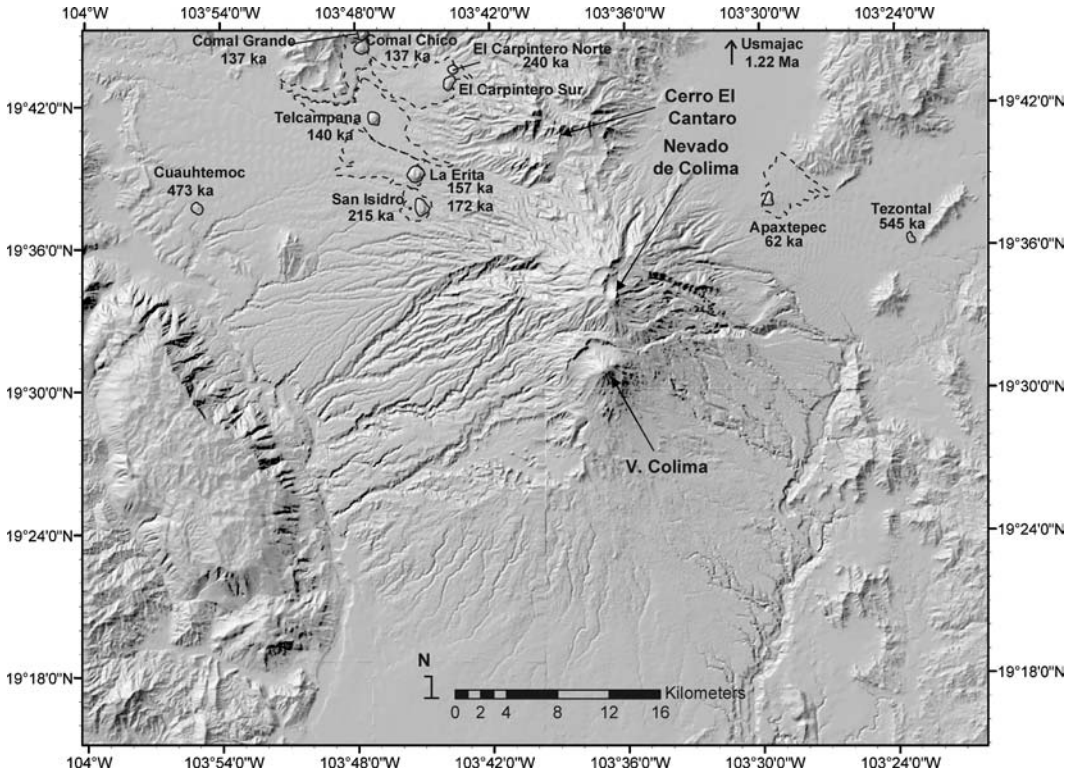

Fig. 2 Shaded hillside digital elevation model (scale 1:20,000) of the Colima volcanic field. Individual cinder cones are outlined in *heavy black lines*, whereas associated lava flows are outlined by *dashed lines*. Ages are shown in kilo years (kyr) and are the isochron ages from Table 3

Chichón in eastern Mexico in 1982 (Luhr et al. 1984). If the scoria cones with associated lavas (e.g., Telcampana, La Erita, El Carpintero Norte, Apaxtepec; Fig. 2) were erupted contemporaneously, it is possible that they released a comparable mass of SO_2 into the atmosphere as the El Chichón eruption. Thus, another goal of this study is to determine both the oxidation states and sulfur concentrations in the scoria and lava erupted from these cones. At the time of the previous study (Luhr and Carmichael 1981), it was not appreciated that analyses of ferric-ferrous ratios in unaltered lava and scoria samples could be used to reveal the equilibrium magmatic oxygen fugacity of the quenched magmas (Carmichael 1991). We use this approach to test whether these alkaline magmas are highly oxidized, and if so, how it affected sulfur behavior prior to and during eruption.

Composition of scoria and lavas

Colima cones

All of the recollected samples from the Colima cones fall within the same petrographic groups found 20 years ago, and are summarized here. The mafic alkaline suite forms a complete transitional range from basanite through leucite-basanite to minette, and the characteristic mineral assemblage of each type is given by Luhr and Carmichael (1981). A strikingly fresh and vesicular lava from La Erita (1015, Table 1) is exposed in a new road cut, so this sample of leucite basanite is an addition to the inventory of samples from the Colima cones. The nomenclature used in 1981 defines basanite as having olivine (Fo_{94}–Fo_{87}, plus chromite) phenocrysts together with less abundant or rare plagioclase and augite phenocrysts. In addition to olivine and augite, the leucite-basanites contain leucite phenocrysts, and the minettes have phlogopite phenocrysts and apatite microphenocrysts.

The two calc-alkaline cones, Tezontal (sample 22E) and Usmajac (sample 1002), are morphologically similar to the alkaline cones, and lie on the northeastern side of the Nevado-Colima volcanic complex (Fig. 2). The Usmajac cone (basaltic andesite) is just off the map in Fig. 2 to the north. The most significant feature of the Tezontal cone is that it erupted basaltic scoria (Table 1), one of the very few young examples of calc-alkaline basalt (<52 wt.% SiO_2) to occur in western Mexico (Luhr et al. 1989). This cone almost completely comprises red oxidized scoria; however, a small outcrop of black scoria was found within the quarry and sampled for this study.

Twelve unaltered, recollected samples from the Colima cones and lavas were analyzed for major and trace elements by X-ray fluorescence (XRF) at the University of California, Berkeley, and the results are reported in Table 1. Previously, multiple samples from each of the cones of Apaxtepec, Telcampana, Comal Chico, San Isidro, and La Erita (Fig. 2) were analyzed by Luhr and Carmichael (1981, see key to sample localities in Appendix 1), and

Table 1 Analyses of scoria and lavas from Pleistocene cinder cones surrounding V. Colima

Sample #	1001B	1003B	1005A	1006B	1007A	1007B	1008B	1013	1015	1016	22E (new)	1002
	lava	lava	scoria	scoria	scoria	lava	lava	lava	lava	lava	scoria	scoria
Latitude	19°37.88’	19°39.60’	19°41.58’	19°44.33’	19°43.60’	19°43.60’	19°45.44’	19°37.39’	19°38.88’	19°37.84’	19°36.45’	19°52.40’
Longitude	103°29.69’	103°45.22’	103°47.23’	103°47.41’	103°43.81’	103°43.81’	103°47.54’	103°45.25’	103°45.58’	103°54.81’	103°23.31’	103°31.97’
Cone	Apaxtepec	La Erita lc	Telcampana	Comal	El Carpintero	El Carpintero	Comal	San Isidro	La Erita lc	Cuahtemoc	Tezontal	Usmajac
Rock type	Basanite	Basanite	Basanite	Chico Basanite	Minette	Minette	Grande Basanite	Minette	Basanite	Basanite	Basalt	Bas Andesite
SiO_2	50.06	48.66	49.18	48.52	48.48	48.41	49.90	48.44	48.77	48.46	49.44	55.18
TiO_2	1.65	1.12	1.04	1.37	1.62	1.63	1.34	1.52	1.30	1.10	0.82	1.40
Al_2O_3	15.99	11.72	12.42	12.38	11.57	11.66	14.42	11.03	11.39	14.13	16.55	16.87
Fe_2O_3	2.87	5.25	5.29	4.30	4.07	4.63	3.54	5.21	4.47	5.08	2.82	2.75
FeO	7.11	2.73	2.79	3.92	3.41	2.91	4.96	2.94	3.56	3.82	6.71	4.86
MnO	0.15	0.12	0.13	0.13	0.12	0.12	0.14	0.12	0.13	0.15	0.15	0.12
MgO	6.15	13.09	13.43	11.54	11.67	11.74	9.08	12.73	13.42	10.57	9.15	4.88
CaO	9.15	9.01	9.02	8.52	8.01	8.07	9.04	8.37	9.35	10.22	10.05	6.95
Na_2O	3.35	2.93	2.56	3.06	3.52	3.76	2.55	2.34	2.28	2.43	2.43	4.03
K_2O	2.20	2.95	3.38	3.35	3.38	2.94	3.55	4.64	3.91	2.58	0.64	1.64
P_2O_5	0.52	1.01	0.83	1.13	1.32	1.31	0.86	1.18	0.95	0.70	0.19	0.44
SO_3	0.01	0.19	0.25	0.04	0.07	0.05	0.02	0.25	0.09	0.03	0.02	0.01
H_2O^+	0.15	0.90	0.20	0.88	1.88	1.87	0.16	0.54	0.26	0.13	0.06	0.41
H_2O^-	0.02	0.26	0.09	0.22	0.29	0.15	0.17	0.22	0.07	0.12	0.12	0.13
Total	99.38	99.94	100.61	99.36	99.41	99.25	99.53	99.53	99.95	99.52	99.15	99.67
Total[a]	99.64	100.47	101.07	99.91	100.34	100.21	99.96	100.10	100.39	99.85	99.23	99.84
S ppm	25	775	1004	165	269	185	99	1003	357	118	93	25
Ni	52	453	430	324	390	358	137	468	401	227	168	76
Cr	99	809	884	606	613	542	424	741	945	572	345	117
Ba	1180	2240	1995	2480	4940	5180	1970	2540	1950	1255	227	552
Rb	22.5	32	20	21	74	74	28	35	29	7	6	18
Sr	1060	2330	2030	2350	3180	3270	1745	2430	1850	1570	496	910
Y	26	20	20	20	29	28	22	21	19	18	21	21
Zr	300	315	256	388	590	590	360	404	329	207	111	192
Mg #	0.61	0.90	0.90	0.84	0.86	0.88	0.77	0.89	0.87	0.83	0.71	0.64
ΔNNO	0.7	4.0	4.0	2.7	2.9	3.6	1.9	3.7	3.0	3.2	1.0	1.5

Notes: Mg#= mol MgO/((MgO + FeO)

[a]Total includes BaO and SrO

considerable variation was found, so it is unlikely that the new analyses given in Table 1 will necessarily reproduce the compositions of each of the cones published by Luhr and Carmichael (1981). To reduce analytical uncertainty, the original wet chemically analyzed samples (Luhr and Carmichael 1981) were used as XRF standards to calibrate the working curves for the new samples.

Mg# (MgO/MgO + FeO) values are high (0.61–0.90), with correspondingly high Ni and Cr contents (52–470 ppm and 99–945 ppm, respectively), indicative of a primary mantle origin for most of the samples (Luhr and Carmichael 1981). K_2O ranges from 2.2–4.6 wt.%, with correspondingly high concentrations in the alkaline samples of Ba (1,200–5,200 ppm), Sr (1,100–3,300 ppm), and Zr (250–600 ppm), which if converted to oxides, and added into the analyses in Table 1, gives totals closer to 100 wt.%. The basanites tend to have lower P_2O_5 (<1 wt.%) than the leucite-basanites, with the minettes typically having 1.2–1.3 wt.% P_2O_5, with TiO_2 following P_2O_5 in this alkaline suite. In Table 1, we also present total sulfur (S) concentrations for each sample. The XRF technique gave a S concentration of 482±4.1 ppm for eight analyses of the standard rock BCR-1, which has a recommended S concentration of 410 ppm. On the basis of multiple analyses, the following precision (±1σ) was obtained: 1004±43 ppm S for sample 1005A and 25±1.7 ppm S for sample 1001B (Table 1).

Potassic lavas adjacent to V. Jorullo

Volcán Colima is close to the Middle America Trench, and in that sense defines the present volcanic front in this part of the Mexican arc (Fig. 1). Historic Volcán Jorullo (1759–1774) defines the volcanic front farther to the east in the state of Michoacán (Fig. 1). The earliest lava associated with this historical eruption is a high-Mg basaltic andesite (Table 2, JOR 44) and successive lavas became increasingly Mg-poor as hornblende became a late-stage phenocryst (Luhr and Carmichael 1985). However, V. Jorullo was preceded by the nearby late-Pleistocene sulfate-rich alkali basalt scoria cone (Cerro La Pilita) and lava (Table 2, JOR 46d). An older cone (unnamed and near Mesa Agua Caliente), which is marginally closer to the Middle America Trench (13 km to the WSW of Cerro La Pilita),

Table 2 Analyes of scoria and lavas from Pleistocene cinder cones surrounding V. Jorullo

Sample #	Mas 2001	Jor 44	Mas 2003a	Jor 46d
	lava	lava	scoria	lava
Latitude	18°56.30′	18°59.49′	18°56.68′	18°55.86′
Longitude	101°50.28′	101°45.14′	101°43.74′	101°44.68′
Cone Rock type	Unnamed basalt	Jorullo Bas. andesite	La Pilita minette	La Pilita trachybasalt
SiO_2	50.44	52.10	49.04	51.72
TiO_2	1.26	0.81	1.31	1.22
Al_2O_3	15.76	16.44	13.46	15.12
Fe_2O_3	3.11	1.56	5.12	4.28
FeO	5.94	6.05	3.17	3.47
MnO	0.14	0.14	0.14	0.12
MgO	8.34	9.29	8.07	8.03
CaO	8.78	8.46	8.73	7.45
Na_2O	3.79	3.47	4.06	4.55
K_2O	1.38	0.74	3.43	2.54
P_2O_5	0.45	0.14	1.59	0.90
SO_3	0.01	0.00	0.59	0.02
H_2O^+	0.13	0.34	0.70	0.43
H_2O^-	0.23	0.10	0.32	0.04
Total	99.76	99.64	99.83	99.89
Total[a]	99.92	99.71	100.44	100.25
S ppm	56	14	2350	98
Ni	189	261	202	221
Cr	306	564	303	329
Ba	545	231	2310	1130
Rb	22	10	8	19
Sr	801	397	3002	1984
Y	22	20	20	18
Zr	150	100	236	183
Mg #	0.71	0.73	0.82	0.80
ΔNNO	1.3	-0.2	3.5	3.0

Notes: Mg#= mol MgO/(MgO + FeO)

[a]Total includes BaO and SrO

Table 3 $^{40}Ar/^{39}Ar$ ages of scoria and lavas associated with Volcán Colima and Volcán Jorullo

Sample	Cinder cone	Total gas age (ka)	Isochron age (ka)	MSWD	$(^{40}Ar/^{36}Ar)_I$	Points fitted	Plateau Age (ka)	MSWD	$\%^{39}Ar$
1002	Usmajac	1216±31	1217±92	1.43	295.4±5.5	13 of 13	1160±26	0.89	75
22E	Tezontal	367±86	545±144	1.38	289.2±4.4	13 of 13	N/A	N/A	N/A
1016	Cuahtemoc	454±14	473±21	2.39	301.2±6.5	13 of 13	449±16	0.48	54
1007A	El Carpintero Norte	257±16	240±27	0.98	303.4±3.9	13 of 13	231±17	0.48	75
1013	San Isidro	109±9	215±18	0.72	294.1±2.9	9 of 13	171±1	0.66	75
1015	La Erita (major cone)	-23±30	157±15	3.30	294.1±2.9	13 of 13	76±29	4.00	80
1003B	La Erita (minor cone)	157±20	172±21	0.71	298.4±3.7	9 of 13	147±16	0.71	80
1005A	Telcampana	155±10	140±13	1.58	297.5±1.1	13 of 13	154±12	1.87	88
1006B	Comal Chico	126±8	137±11	0.82	311.6±8.2	13 of 13	110±8	0.11	70
1008B	Comal Grande	99±8	137±12	0.33	297.6±5.8	13 of 13	105±7	0.34	100
1001B	Apaxtepec	82±15	62±14	2.90	298.5±1.1	13 of 13	51±5	0.13	58
1004-500	Apaxtepec	40±19	53±14	1.72	288.2±7.5	13 of 13	66±18	1.49	87
Mas 2001	Unnamed	1110±27	1060±47	1.41	304.5±12.6	13 of 13	1080±24	1.34	96
Jor 46d	Cerro La Pilita	160±18	102±20	0.64	298.4±2.0	13 of 13	160±15	0.77	100

All errors are reported as 1 sigma. Monitor was Fish Canyon Tuff biotite-split 3 (27.99 Ma)
Latitude and longitude of specimens are given in Tables 1 and 2. Preferred ages are isochron ages

erupted basalt with 1.4 wt.% K_2O (Table 2, MAS 2001). The compositions of these two basalts (*sensu lato*) reflect one of the curiosities of the pattern of volcanism in the west-central Mexican Volcanic Belt, namely the tendency for contemporaneous lavas close to the volcanic front to be enriched in K_2O relative to those farther from the trench (Blatter et al. 2001).

$^{40}Ar/^{39}Ar$ geochronology

Methods

Ages for 11 Colima cones and two scoria cones near V. Jorullo were determined by the $^{40}Ar/^{39}Ar$ laser ablation step-heating method and are given in Table 3. All analyses were run at the University of Michigan, and the procedures closely followed those described in Hall and Farrell (1995) and Frey et al. (2004). Samples were taken from the interiors of lava flows or the inner cores of dense volcanic bombs from cinder cones, and each sample was checked for alteration using a petrographic microscope. For each sample, groundmass separates were handpicked for irradiation with fast neutrons for 6 h at the Phoenix-Ford Memorial Reactor at the University of Michigan. Fish Canyon Tuff biotite split-3 (FCT-3) was used as a neutron-fluence monitor and yielded a K-Ar age of 27.99±0.04 Ma (2 sigma), relative to 520.4 Ma for MMhb-1 (Hall and Farrell 1995; Samson and Alexander 1987). This age is comparable to the 28.02±0.09 Ma age reported by Renne et al. (1998). Additional details of the procedures that were followed are given in Frey et al. (2004).

Results

The $^{40}Ar/^{39}Ar$ data analysis for each sample, including gas spectra and inverse isochron diagrams, are given as Electronic Supplementary Material (ESM Figs. 1–4). A summary of this information along with total gas, isochron, and plateau ages is reported in Table 3. The error analysis for each sample includes uncertainties in peak signals, system blanks, spectrometer mass discrimination, reactor corrections, and *J* values. The error on the plateau age is a standard weighted error for the individual steps by variance (Taylor 1982), i.e., release fractions with more precise results carry greater weight in the age calculation. All but one sample (22E, Tezontal) gave $^{40}Ar/^{39}Ar$ release spectra that resulted in a plateau. The isochron ages for all but one (1013, San Isidro) of these 12 samples are within two sigma error of their respective plateau ages. The preferred ages for the samples in Table 3 are the isochron ages, where all but three have MSWDs <1.8 (ranging from 0.33 to 3.30).

As a check on our $^{40}Ar/^{39}Ar$ method, two different samples from the morphologically youngest scoria cone, Apaxtepec, were dated. The first sample (1004-500; Table 3) is

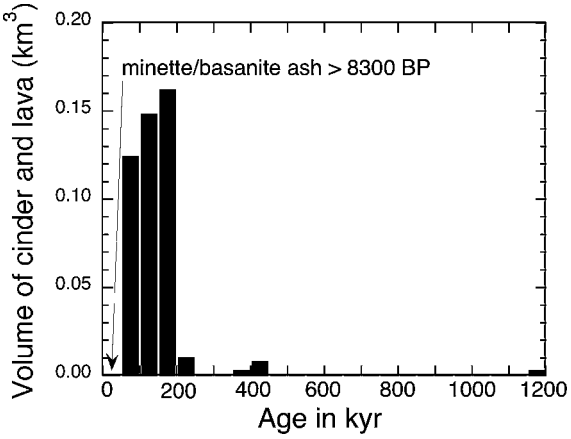

Fig. 3 Volumes of lava and scoria, uncorrected to magma equivalent, for the Colima cones plotted against ages of eruptions (Tables 3 and 5)

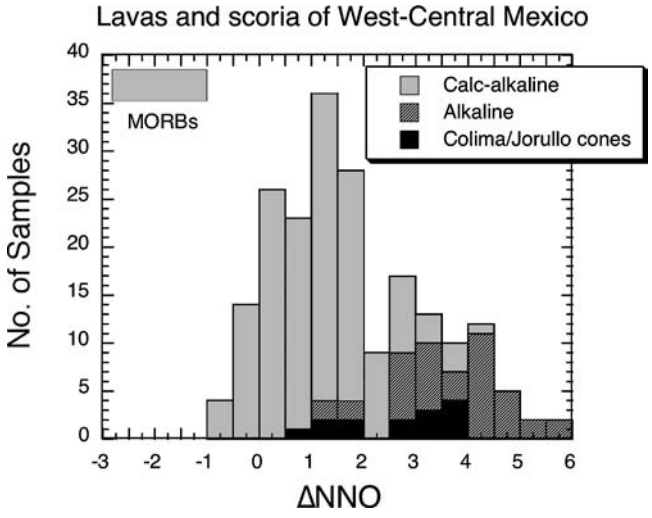

Fig. 4 Plot of ΔNNO calculated as described in the text using the analyzed FeO and Fe_2O_3 contents of lavas. Data are taken from Tables 1 and 2, Blatter and Carmichael (1998, 2001), Carmichael et al. (1996), Hasenaka and Carmichael (1987), Luhr and Carmichael (1980, 1981, 1985), Wallace and Carmichael (1999). Data for MORBs are taken from Christie et al. (1986) and Wallace and Carmichael (1992b); there are far more than ~ 30 samples of MORBs

that collected by Luhr and Carmichael (1981), whereas the second sample (1001B; Table 3) was collected more than 20 years later. In addition, the two samples were irradiated and laser heated more than 18 months apart. The results give isochron ages (53±14 ka; 62±14 ka) that average to 58±10 ka and plateau ages (66±18 ka; 55±5 ka) that average to 59±9 ka. The dates on the two specimens are fully consistent with each other and indicate an eruption age for the Apaxtepec cone at ~60 ka.

Of the 11 Colima cones, the two oldest are the calc-alkaline types, the basaltic andesite from the Usmajac cone (1217±92 ka) and the basalt from Tezontal cone (545±144 ka). The next eruption produced basanite at the Cuahtemoc cone at 473±21 ka. After a hiatus of ~200 kyr, minette erupted as scoria and lava at El Carpintero Norte at 240±27 ka. Between ~200 and ~60 ka, the remaining potassic cones and associated lavas were erupted. The most potassic magma of the Colima cones (minette with 4.64 wt.% K_2O) was erupted at San Isidro at 215±18 ka. Next, the major and minor cones of La Erita were erupted (157±15 ka; 172±21 ka); these $^{40}Ar/^{39}Ar$ ages (and 1σ errors) suggest that these two cones, both of which produced leucite basanite, may have erupted contemporaneously. The average of their dates (~165±13 ka) likely gives a better estimate of their eruption age, which is close to that for the basanite from Telcampana cone (140±13 ka). Similarly, the Comal Chico and Comal Grande cones, which erupted basanite magmas of distinctly different composition (Table 1), have indistinguishable eruption ages (137±11 ka; 137±12 ka). The youngest cone, Apaxtepec, erupted at ~60 ka, as discussed above.

The two samples of potassic basalt near the historically active cone of V. Jorullo at the volcanic front, ESE of the Colima graben (Fig. 1), were erupted ~ 1 Myr apart. The unnamed scoria cone near Mesa Agua Caliente (MAS-2001) has an isochron age of 1060±47 ka and a plateau age of 1080±24 ka, whereas Cerro La Pilita (JOR 46d) has an isochron age of 102±20 ka and a plateau age of 160±15 ka (Table 3).

Eruption volumes for Colima cones and associated lavas

Twenty years ago, the volumes of the cinder cones surrounding Volcán Colima were estimated using geometric simplifications of cones emplaced on horizontal plane surfaces. It is now possible to more accurately calculate volumes of cones and lavas using digital elevation models (DEM) and ortho airphotos as described by Frey et al. (2004). The DEMs and orthophotos use a Universal Transverse Mercator (UTM) projection and the Geodetic Reference System 80 (GRS 80) geodetic model. The lateral and vertical resolution of the DEMs is 50 and 2 m, respectively, based on a 1:50,000 scale, whereas the orthophotos are based on a 1:20,000 scale and have a resolution of 2 m/pixel. The margins of each cinder cone and associated lava flow were digitized on the orthophotos with the aid of geologic field maps, topographic maps, and Landsat images. From the digitized margins, a three-dimensional representation of the surface topography was created. Cone and lava volume were calculated by the difference of a linear interpolation of this surface and a base level determined from the surrounding topography.

In attempting to quantify eruptive volumes from the cinder cones, an assessment of errors is required. One source of error is the effect of degradation and removal of scoria via erosion over the last 1 Myr. The Colima cinder cones, most of which (8 of 11) are younger than 250 ka, range from having smooth flanks to being dissected by small gullies and rills. According to Colton's (1967) scheme of cinder cone degradation, they are classified as stage 5 (youngest) to stage 3 (moderate). Morphometric studies (e.g., Colton 1967; Wood 1980) of cinder cone degradation show that cone heights, height/basal diameter ratios, and flank slopes decrease with cinder cone age. However, crater diameter/basal diameter ratios appear independent of degradation (and composition), suggesting that erosion removes the top of the cone and mass-wasting processes deposit material at the base of the cinder cone (Wood 1980). A compilation of basal and crater diameters and heights for the 11 Colima cones is given in Table 4. For all cones erupted ≤250 ka (8 of 11), both the height/basal diameter ratios and the crater diameter/basal diameter ratios are very similar. So, although the shapes of cinder cones may change with time, their volumes (as captured by our GIS methods) are conserved to first order.

Another source of error is the amount of tephra erupted from the cones that fell beyond the base of the cone. In the case of the highly explosive Parícutin eruption in Mexico (type example of violent strombolian activity from a cinder cone; Walker 1973), Fries (1953) determined that the volume of tephra that fell beyond Parícutin extended to 8 times the volume of the cone. In contrast, mapped

Table 4 Dimensions and volumes of cinder cones

Cinder cone	H (m)	BD (m)	CD (m)	H/BD	CD/BD	Vol (km^3)
Apaxtepec	90	700	250	0.13	0.36	0.013
Comal Chico	150	1,050	410	0.14	0.39	0.029
Comal Grande	180	950	285	0.19	0.30	0.032
Telcampana	160	935	335	0.17	0.36	0.008[c]
La Erita (major)	260	1,335	485	0.19	0.36	0.073
San Isidro	200	1,200	450	0.17	0.38	0.046
El Carpintero N	140	735	275	0.19	0.38	0.010
El Carpintero S	135	975	220/160[b]	0.15	0.39[b]	0.027
Cuahtemoc	60	925	225	0.06	0.24	0.008
Tezontal	50	685	130	0.08	0.19	0.003
Usmajac[a]	60	–	–	–	–	0.003

Abbr.: *H* height, *BD* basal diameter, *CD* crater diameter

[a]Data from Luhr and Carmichael (1981)

[b]Two nested craters; two crater diameters are given; their sum is used to calculate CD/BD

[c]Includes volume estimate for associated surge beds

tephra blankets elsewhere (e.g., Holocene cinder cones at Newberry Volcano, Oregon; MacLeod et al. 1995) amount to a small fraction of the cone volumes. It is not known whether the eruptions of the Colima cones were characterized by violent strombolian activity, like Parícutin, or were less energetic; any distal tephra deposits laid down >60 kyr ago are now covered by soil and vegetation, and are not mapped. Nonetheless, we can use the Parícutin example as an upper bound for our volume estimates.

The calculated volumes of the 11 Colima cones are given in Table 4. The Usmajac cone, which is located off the map in Fig. 2, has an estimated volume of 0.003 km^3 from Luhr and Carmichael (1981), which we have added to Table 4. The total volume of these 11 scoria cones is 0.25 km^3, similar to the estimate of 0.19 km^3 given by Luhr and Carmichael (1981). The two largest cones are La Erita and San Isidro (0.07 and 0.05 km^3), whereas the two smallest (and also the two oldest in Fig. 2) are Cuahtemoc and Tezontal (0.008 and 0.003 km^3). One of the cones, Telecampana, has associated surge beds; their volume is estimated to be ~5–20% of that of the cone itself. To convert the scoria cone volumes to a dense magma equivalent, the effect of vesicularity and the packing of the scoria clasts must be considered. Thus an estimate of the minimum volume of magma erupted as scoria is ~25% of the total volume of the 11 cones, namely ~0.06 km^3. The maximum is the total volume with no correction applied, although we take 50% as a more realistic upper bound on the dense magma equivalent, namely ~0.12 km^3. However, if this estimate is multiplied by 8, to account for any tephra that fell well away from the respective cones on a scale similar to that at Parícutin, then we obtain an upper limit of 0.96 km^3.

Alkaline magma from the Colima cones erupted not only as scoria, but also as associated lava flows. In Table 5, the area of each lava flow field (a set of flows associated with individual cones; Fig. 2) is given, along with a maximum, minimum, and best estimate for the total volume of each set of flows. The total volume is estimated to range from 0.2 to 1.5 km^3 (minimum and maximum), with best estimates for individual flow fields that total to ~0.8 km^3. Once again, the relative errors on these estimates are large, but the total volumes are sufficiently low compared to the central andesitic volcanism in the Colima graben that robust conclusions contrasting the eruption rates can be drawn (see discussion section). Luhr and Carmichael (1981) do not break down their volume estimates for the various lava flows, but give a total estimate of ~0.2 km^3, which is our minimum volume.

Discussion

Ages, volumes, and eruption rates

Although the morphological ages of the Colima cones estimated by Luhr and Carmichael (1981, Table 1) were all $\leq$ 40 ka, the ^{40}Ar/^{39}Ar dates in Table 3 range from 1.2 Ma to 60 ka. Nonetheless, the relative ages of the cones given by Luhr and Carmichael (1981) are consistent with the ^{40}Ar/^{39}Ar results. The oldest dated cone (Usmajac, 1217±92 ka), NE of Volcan Colima (Fig. 2) is indeed the cone estimated by Luhr and Carmichael (1981) to be the oldest. The oldest cone on the west side of Volcán Colima, Cuauhtemoc (Fig. 2; 473±21 ka, Table 3), is the only cone that has lake sediments on its lower flanks, but we know

Table 5 Volume of lava flow fields associated with cinder cones

Cinder cone	Area (km^2)	Range in thickness (m)	Min volume (km^3)	Max volume (km^3)	Best estimate (km^3)
Apaxtepec	13.42	2–9	0.03	0.12	0.05
Telcampana	21.87	2–20	0.04	0.43	0.21
Comal Chico	10.28	2–16	0.02	0.16	0.12
Comal Grande	1.99	5–10	0.01	0.02	0.02
El Carpintero	18.22	2–14	0.04	0.26	0.15
La Erita	17.25	2–21	0.03	0.37	0.18
San Isidro	4.26	2–26	0.01	0.11	0.06
Total			0.17	1.47	0.79

that this lake, or its marshy successor, existed at the time that Telecampana (1005A, 140±13 ka) erupted because of the occurrence of associated surge beds that are deposited on lake/marsh deposits (Luhr and Carmichael 1981).

The most voluminous of the potassic lavas and scoria, made of minette, leucite-basanite and basanite, all erupted in the interval of ~240–60 ka (Fig. 3; Table 3), which overlaps the period during which calc-alkaline andesites are known to have erupted from the nearby central volcano of Nevado de Colima (Robin et al. 1987); it is presumably the period during which the andesitic cone of the presently active Volcán Colima was being built. Our best estimate for the total volume of potassic magma erupted over the last 250 kyr is ~1.3 km^3, which leads to an eruption rate of ~0.005 km^3/kyr. This rate is more than 200 times lower than the cone-building eruption rate of ≥1.2 km^3/kyr for the historically active Volcán Colima, which has produced at least 5 km^3 of lava (predominantly andesite) over the last 4.3 kyrs (Luhr and Prestegaard 1988). If the entire history of the Colima cones over the last 1.2 Myr is considered, then the total erupted volume is only incrementally larger at ~1.4 km^3, which leads to an average eruption rate of ~0.001 km^3/kyr or ~1.2 km^3/Myr. This is ~4 times greater than the eruption rate of ~0.3 km^3/Myr for lamproite (highly potassic) lavas at the Leucite Hills in Wyoming (Lange et al. 2000), but it is 400–800 times lower than the rate at which andesite/dacite has erupted from the Colima-Nevado complex over the last 1 Myr.

A detailed examination of the ash and scoria deposits on the upper flanks of Volcán Colima by Luhr and Carmichael (1982) showed that basanite/minette magma intermingled with andesitic magma at ~8.3 ka. These mixed ashes and scoria were preceded by a thick (3 m) basanite ash horizon on the volcano that puzzled those authors because of the distances to the most likely young alkaline cones that could be the source of these ashes (La Erita or Cuauhtemoc, 20 and 35 km, respectively; Fig. 2). The new dates (Table 3) establish unequivocally that the mingling of basanite/minette and andesite magma revealed in the ash horizons of Volcán Colima, and the underlying basanite ash layer, are much younger than the nearby scoria cones. Thus, the basanite/minette magma is not from one of these cones, but likely used the fracture system and central vent of Volcán Colima for eruption. Given the number of alkaline eruptions in the Colima graben over the last 250 kyr, it is reasonable to expect that this magma type will erupt again, either through the same fracture system feeding Volcán Colima and/or to form another neighboring cone.

Oxidation state of potassic magmas and sulfur release on eruption

Oxygen fugacity

In this study, a considerable effort was made to sample fresh unaltered scoria and lava so that the ferric-ferrous ratio of each sample could be used to calculate a magmatic oxygen fugacity. For all the samples reported in Tables 1 and 2, the olivine phenocrysts are pale-green in hand specimens and are without any sign of alteration in thin section (e.g., no bowlingite or iddingsite along the olivine rims). The composition of the olivine phenocrysts in a series of unaltered, Quaternary lavas from Mascota have been shown to be in FeO-MgO exchange equilibrium with the host magma by Carmichael et al. (1996), thus confirming the premise that the ferric-ferrous ratios of Quaternary samples, without signs of alteration in thin section, represent magmatic values.

In a multi-component silicate liquid, the ratio Fe_2O_3/FeO is a function of temperature, composition, and oxygen fugacity at 1 bar. The iron redox state is related to these parameters by the empirical relation:

$$\ln [X_{Fe_2O_3}/X_{FeO}] = a \ln f_{O_2} + b/K + c + \Sigma X d_i$$

where a, b, c and d_i are constants derived by regression of a range of silicate liquids equilibrated from air to the I–W (Fe-FeO) oxygen buffer, over a range of temperatures at 1 bar (Sack et al. 1980; Kilinc et al. 1983; Kress and Carmichael 1988, 1991). Using values of FeO and Fe_2O_3 determined by wet chemistry (Table 1), a value of $\ln f_{O_2}$ can be calculated at 1,200 °C, and from this value, the oxygen fugacity defined by the buffer Ni-NiO has been subtracted at the same temperature. The result (ΔNNO) is independent of temperature, and provided that the lava is unaltered (see discussion below), the value will reflect the equilibrium oxygen fugacity required to support the observed redox ratio. The pressure dependence of the oxygen fugacity is small at low pressures (Kress and Carmichael 1991) and has been omitted. Values of oxygen fugacity obtained by this method for Hawaiian lavas are in excellent agreement with those obtained by analyses of volcanic gases (Gerlach 1993), with those obtained from the compositions of coexisting Fe-Ti oxides (Carmichael 1991), and with those obtained from Mössbauer spectroscopy on synthetic basaltic liquids and glasses (Partzsch et al. 2004).

The values of ΔNNO for the scoria and lavas from the various Colima cones are given in Table 1 and are plotted in Figs. 4 and 5. The new ferric-ferrous analyses for most of the basanite, leucite-basanite, and minette samples (Table 1) lead to ΔNNO values between 2 and 4, which are similar to those obtained for the olivine minette lavas from the Mascota volcanic field (Carmichael et al. 1996). This range is about two orders of magnitude higher than is typical of calc-alkaline arc magmas from west-central Mexico (Fig. 4). The one exception is the basanite from the Apaxtepec cone, the youngest of all the Colima cones, which has a ΔNNO value of 0.7. The new leucite basanite sample taken from a recent road cut (sample 1015 from La Erita) is strikingly fresh, and its ΔNNO value of 3.0 is very likely pristine. In Fig. 5, a plot of ΔNNO vs. Ba is shown for all the samples from this study (all olivine-bearing) as well as the olivine minettes and basaltic andesites (all olivine-bearing) from the Quaternary Mascota field (Lange and Carmichael 1990; Carmichael et al. 1996). The positive correlation between ΔNNO and Ba strongly suggests that the redox state of the Colima cones reflects

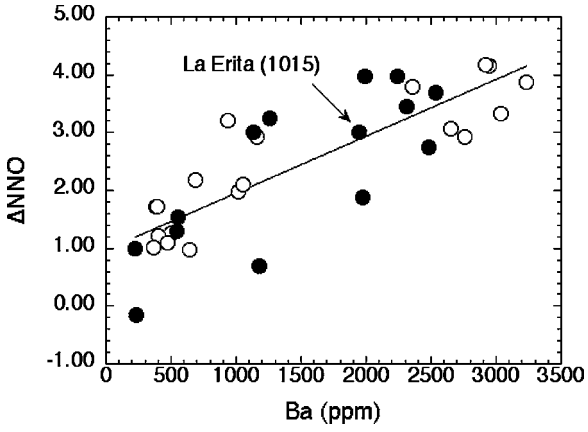

Fig. 5 Plot of ΔNNO vs. Ba (ppm) for all samples in Tables 1 and 2 (*solid circles*) and olivine-bearing minettes and basaltic andesites (*open circles*) from Mascota (Carmichael et al., 1996). The linear regression to the data shows a positive correlation between ΔNNO and Ba concentration, both of which reflect the influence of slab-derived fluids. The freshest sample collected in this study (La Erita, sample 1015) has a ΔNNO value of 3.0, which closely represents the pre-eruptive magmatic value and not the effects of post-eruptive weathering

the influence of a highly oxidized, slab-derived fluid, which probably formed phlogopite-bearing veins within the sub-arc mantle (Carmichael et al. 1996). Therefore, the ΔNNO values of 2–4 for the potassic magmas erupted from the Colima cones represent, to first order, magmatic values and are not the result of post-eruptive weathering and oxidation.

The most significant change from the results given in Luhr and Carmichael (1981) is for sample 22E, one of the few basalts in western Mexico, which comes from the pervasively oxidized Tezontal scoria cone. After a lengthy search we found a rare example of a dense black core in a volcanic bomb, which was analyzed (Table 1). This unoxidized sample is more reduced (ΔNNO=1.0) than the original, thoroughly red and oxidized sample (ΔNNO=2.5) analyzed by Luhr and Carmichael (1981). We consider this lower oxidation state to be more representative of the rare examples of Quaternary basaltic magma in western Mexico.

Sulfur concentration and release on eruption

A wide variety of experiments in the literature show that sulfur solubility in silicate liquids is a strong function of oxidation state and that sulfur dissolves primarily as sulfate species under oxidizing conditions (>Ni-NiO buffer) (Carroll and Webster 1994). Moreover, under these oxidizing conditions, the solubility of sulfur increases with oxidation state (Katsura and Nagashima 1974). Thus it is plausible that the highly oxidized magmas erupted from the Colima cones may have contained substantial concentrations of dissolved sulfate.

Although sulfur is presently being deposited in the active summit crater of Volcán Colima, sulfur-bearing minerals are rare in Quaternary calc-alkaline volcanic rocks from western Mexico, although pyrrhotite has been found in a series of high-Mg andesites from central Mexico (Blatter and Carmichael 2001). Alkaline magmas, particularly minettes (Carmichael et al. 1996) and trachybasalts (Luhr and Carmichael 1985; Barclay and Carmichael 2004) often have microphenocrysts of apatite, so that part of the magmatic sulfur will be retained on eruption, because sulfate is incorporated in the apatite structure (Peng et al. 1997; Parat and Holtz 2004). Two apatite crystals in Colima leucite-basanites contain 1.21 and 0.96 wt.% SO_3 (Luhr and Carmichael 1981), greater than the amount found in apatite (0.34 wt.%) coexisting with anhydrite and pyrrhotite in the trachyandesite scoria of the 1982 eruption of El Chichón, SE Mexico (Luhr et al. 1984). However anhydrite, which accounts for the majority of the S in fresh El Chichón pumices, has not yet been found (as of 2005) in any young volcanic rocks from west-central Mexico. The SO_3 contents of the analyzed Colima alkaline samples are given in Table 1, and despite the large concentrations in the apatite phenocryst analyses noted above, the levels in the lavas are always less than 0.25 wt.%, far lower than the amount (1.2 wt.%) in the fresh El Chichón pumices (Luhr et al. 1984). However, we note that Maria and Luhr (2004) analyzed up to 2.3 wt.% SO_3 in olivine melt inclusions in minette and basanite scoria from Mascota and Colima cones. The highest concentration of whole-rock SO_3 so far found in western Mexico is 0.59 wt.% for biotite-bearing trachybasalt bombs (MAS 2003a, Table 2; Barclay and Carmichael 2004) from the Pleistocene cone Cerro La Pilita, close by the historically (1759–1774) active Volcán Jorullo (Luhr and Carmichael 1985).

Eruptions of anhydrite-bearing magmas at El Chichón (Luhr et al. 1984) and Pinatubo (Westrich and Gerlach 1992, Gerlach et al. 1996) were accompanied by large

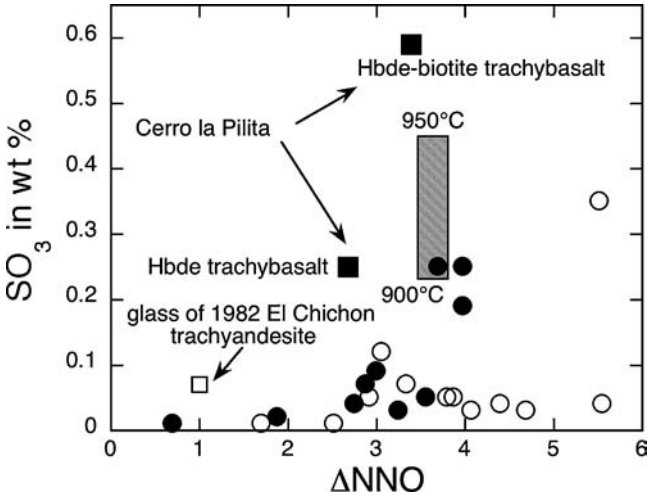

Fig. 6 Plot of ΔNNO against measured S concentrations, calculated as SO_3 in alkaline lavas from west-central Mexico. The ornamented rectangle shows the range of SO_3 solubilities in liquids equilibrated with anhydrite at ΔNNO ~3.6 (Mn_3O_4-MnO buffer, hausmannite-manganosite) at two different temperatures at 2 kb for a basaltic andesite from Volcan Jorullo (Luhr 1990). Data are taken from Tables 1 and 2, and unpublished analyses of S in alkaline lavas from Mascota, western Mexico (Carmichael et al. 1996)

injections of SO_2 into the atmosphere, estimated at 7 and 20 megatons respectively (Bluth et al. 1992). Thus the question arises about the sulfate concentration of these alkaline magmas from west-central Mexico, and whether they were saturated with anhydrite (or emitted significant amounts of SO_2) on the day of their eruption. Anhydrite is stable at relatively high oxygen fugacities, ΔNNO>1.0–1.5, (Carroll and Rutherford 1987) and anhydrite-saturated magmas worldwide have the following features: they are highly oxidized, crystal-rich, fluid saturated, with abundant hornblende or biotite (Peng et al. 1997). However, anhydrite rarely survives in the geologic record as it is very soluble in water and can disappear from surface flows after several rainstorms.

From the data reported in Carroll and Webster (1994), magmas with values of ΔNNO>1 will have 80% or more of the sulfur dissolved as sulfate. Thus we have plotted measured concentrations of S, calculated as SO_3, against ΔNNO for these alkaline lavas (Tables 1, 2) and compared them to El Chichón in Fig. 6. The data in Fig. 6 include the SO_3 content of the matrix glass of El Chichón, which was in equilibrium with anhydrite, and the sulfate solubilities in a basaltic andesite (Table 2, JOR 44) at 900–950 °C in equilibrium with anhydrite (Luhr 1990). A plausible speculation from these SO_3 concentrations (and the melt inclusion study of Maria and Luhr 2004) is that the alkaline magmas, prior to eruption, had substantial amounts of dissolved SO_3 at levels appropriate to stabilize anhydrite. However, whether anhydrite was ever present in the scoria or lavas remains an open question.

Nevertheless, it is conceivable that significant amounts of SO_2 were released to the atmosphere by the eruption of the Colima alkaline magmas. Although their aggregate volume (Table 4) exceeds that of the 1982 El Chichón eruption (~0.4 km^3), the precision of their measured ages (Table 3) shows that they were erupted episodically over a prolonged time interval (~180 kyr; Fig. 3), so that there was a sequential rather than an abrupt release of sulfur gases to the atmosphere. As the solubility of sulfur in basic magmas is a strong function of oxygen fugacity (Katsura and Nagashima 1974), with a solubility minimum at ΔNNO=0, highly oxidized alkaline magmas associated with subduction are the principal means of transporting sulfur (as sulfate) from the modified mantle wedge to the Earth's atmosphere.

Acknowledgements The XRF analyses were made by Laura Glaser and Tim Teague of UC Berkeley, and the development of the procedure to measure S in these samples is due to them. We thank Marcus Johnson for his assistance in the Ar geochronology lab at the University of Michigan. Insightful comments by Jim Luhr, Mac Rutherford, and Julie Donnelly-Nolan substantially improved this manuscript. This research was supported the National Science Foundation: EAR-0228919 to ISEC and EAR-9909567 to RAL

Appendix

Table A Key to sample numbers

Cinder cone	Sample # (this study)	Description (this study)	Sample # (LC 1981)	Description (LC 1981)
Apaxtepec	1001B	lava from associated flow	1004–500/501	scoria from cone
Usmajac	1002	dense interior of bomb from scoria cone	SAY 17B	dense bomb from scoria cone
La Erita (minor cone)	1003B	lava (not scoria) from minor cone	SAY 5A	lava underlying scoria
Telcampana	1005A	massive lava from cone	1004-507/508	scoria from cone
Comal Chico	1006B	dense interior of bomb from scoria cone	SAY 8G/8H	scoria from cone
El Carpintero Norte	1007A	dense interior of bomb from scoria cone	SAY 7E	scoria from cone
El Carpintero Norte	1007B	lava flow from cone	SAY 7E	scoria from cone
Comal Grande	1008B	lava block from cone	not sampled	
San Isidro	1013	dense interior of bomb from scoria cone	SAY 6A,6D, 6E	scoria from cone
La Erita (main cone)	1015	vesicular lava from main cone	1004–511	large bomb among cinder
Cuauhtemoc	1016	lava from cone	1004–510	scoria from cone
Tezontal	22E	dense bomb analyzed; lava flow dated	SAY 22E	dense bomb from scoria cone

LC (1981) is Luhr and Carmichael (1981)

References

Allan JF (1986) Geology of the northern Colima and Zacoalco grabens, southwest Mexico: Late-Cenozoic rifting of the Mexican volcanic belt. Geol Soc Am Bull 97:473–485

Barclay J, Carmichael ISE (2004) A hornblende basalt from western Mexico: water-saturated phase relations constrain a pressure-temperature window of eruptibility. J Petrol 45:485–506

Blatter DL, Carmichael ISE (1998) Plagioclase-free andesites from Zitacuaro (Michoacan), Mexico: petrology and experimental constraints. Contrib Mineral Petrol 132:121–138

Blatter DL, Carmichael ISE (2001) Hydrous phase equilibria of a Mexican high-silica andesite: A candidate for a mantle origin? Geochim Cosmochim Acta 65:4043–4065

Blatter DL, Carmichael ISE, Deino AL, Renne PR (2001) Neogene volcanism at the front of the central Mexican volcanic belt: basaltic andesites to dacites, with contemporaneous shoshonites and high-TiO_2 lava. Geol Soc Am Bull 113:1324–1342

Bluth GJ, Doiron SD, Schnetzler CC, Krueger AJ, Walter LS (1992) Global tracking of the SO_2 clouds from the June, 1991 Mount Pinatubo eruptions. Geophys Res Lett 19:151–154

Carmichael ISE (1991) The redox states of basic and silicic magmas: A reflection of their source regions? Contrib Mineral Petrol 106:129–141

Carmichael ISE, Lange RA, Luhr JF (1996) Quaternary minettes and associated volcanic rocks of Mascota, western Mexico: a consequence of plate extension above a subduction modified mantle wedge. Contrib Mineral Petrol 124:302–333

Carroll MR, Rutherford MJ (1987) The stability of igneous anhydrite: experimental results and implications for sulfur behavior in the 1982 El Chichon trachyandesite and other evolved magmas. J Petrol 28:781–801

Carroll MR, Webster JD (1994) Solubilities of sulfur, noble gases, nitrogen, chlorine and fluorine in magmas. In: Carrol MR, Holloway JR (eds) Volatiles in Magmas. Rev Mineral 30:231–279

Christie DM, Carmichael ISE, Langmuir CH (1986) Oxidation states of mid-ocean ridge basalt glasses. Earth Planet Sci Lett 79:397–411

Colton HS (1967) Cinder cones and lava flows. Museum of Northern Arizona, Flagstaff, Arizona, pp 1–58

Delgado Granados H. (1993) Late Cenozoic tectonics offshore western Mexico and its relation to the structure and volcanic activity in the western Trans-Mexican Volcanic Belt. Geofís Int 32:543–559

DeMets C Stein S (1990) Present-day kinematics of the Rivera plate and implications for tectonics in southwestern Mexico. J Geophys Res 95:21931–21948

Fries C (1953) Volumes and weights of pyroclastic material, lava, and water erupted by Parícutin volcano, Michoacán, Mexico. Trans Am Geophys Union 34:603–616

Frey HM, Lange RA, Hall CM Delgado Granados H (2004) Magma eruption rates constrained by $^{40}Ar/^{39}Ar$ chronology and GIS for the Ceboruco-San Pedro volcanic field, western Mexico. Geol Soc Am Bull 116:259–276 (Errata 116:1040)

Gerlach TM (1993) Oxygen buffering of Kilauea volcanic gases and the oxygen fugacity of Kilauea basalt. Geochim Cosmochim Acta 57:795–814

Gerlach TM, Westrich HR, Symonds RB (1996) Preeruption vapor in magma of the climactic Mount Pinatubo eruption: source of the giant stratospheric sulfur dioxide cloud. In: Newhall CG, Punongbayan RS (eds) Fire and mud: eruptions and lahars of Mount Pinatubo, Philippines. University of Washington Press, Seattle, 415–433

Hall CM, Farrell JW (1995) Laser $^{40}Ar/^{39}Ar$ ages of tephra from Indian Ocean deep-sea sediments: tie points for the astronomical and geomagnetic polarity time scales. Earth Planet Sci Lett 133:327–338

Hasenaka T, Carmichael ISE (1987) The cinder cones of Michoacan-Guanajuato, central Mexico: petrology and chemistry. J Petrol 28:241–269

Johnson CA, Harrison CGA (1990) Netectonics in central Mexico. Phys Earth Planet Int 64:187–210

Katsura T, Nagashima S (1974) Solubility of sulfur in some magmas at 1 atmosphere. Geochim Cosmochim Acta 38:517–531

Kilinc A, Carmichael ISE, Rivers ML, Sack RO (1983) The ferric-ferrous ratio of natural silicate liquids equilibrated in air. Contrib Mineral Petrol 83:136–140

Kress VC, Carmichael ISE (1988) Stoichiometry of the iron oxidation reaction in silicate melts. Am Mineral 73:1267–1274

Kress VC, Carmichael ISE (1991) The compressibility of silicate liquids containing Fe_2O_3 and the effect of composition, temperature, oxygen fugacity and pressure on their redox states. Contrib Mineral Petrol 108:82–92

Lange RA, Carmichael ISE (1990) Hydrous basaltic andesites associated with minette and related lavas in western Mexico. J Petrol 31:1225–1259

Lange RA, Carmichael ISE Hall CM (2000) $^{40}Ar/^{39}Ar$ chronology of the Leucite Hills, Wyoming: eruption rates, erosion rates, and an evolving temperature structure of the underlying mantle. Earth Planet Sci Lett 174:329–340

Luhr JF (1990) Experimental phase relations of water-saturated and sulfur-saturated arc magmas and the 1982 eruptions of El Chichón Volcano. J Petrol 31:1071–1114

Luhr JF, Carmichael ISE (1980) The Colima volcanic complex, Mexico: Part I. post-caldera andesites from Volcan Colima. Contrib Mineral Petrol 71:343–372

Luhr JF, Carmichael ISE (1981) The Colima Volcanic complex, Mexico: Part II. Late Quaternary cinder cones.. Contrib Mineral Petrol 76:127–147

Luhr JF, Carmichael ISE (1982) The Colima volcanic complex, Mexico: Part III. ash and scoria fall deposits from the upper slopes of Volcan Colima. Contrib Mineral Petrol 80:262–275

Luhr JF, Carmichael ISE (1985) Jorullo volcano, Michoacan, Mexico (1759–1774): the earliest stages of fractionation in calc-alkaline magmas. Contrib Mineral Petrol 90:142–161

Luhr JF, Prestegaard KL (1988) Caldera formation at Volcano Colima, Mexico by a large Holocene volcanic debris avalanche. J Volcanol Geoth Res 35:335–348

Luhr JF, Carmichael ISE, Varekamp JC (1984) The 1982 eruptions of El Chichon volcano, Chiapas, Mexico: mineralopy and petrology of the anhydrite-bearing pumices. J Volcanol Geotherm Res 23:69–108

Luhr JF, Allan JF, Carmichael ISE, Nelson SA Hasenaka T (1989) Primitive calc-alkaline and alkaline rock types from the western Mexican Volcanic Belt. J Geophys Res 94:4515–4530

MacLeod NS, Sherrod DR, Chitwood LA, Jensen RA (1995) Geologic map of Newberry volcano, Deschutes, Klamath,and Lake Counties, Oregon. USGS Map I-2455

Maria AH, Luhr JF (2004) Melt inclusions in Late-Quaternary basanites and minettes of the Colima Rift and Mascota Volcanic Field (western Mexican Volcanic Belt). In: Aguirre-Díaz GJ, Macías-Vásquez JL, Siebe C (eds) Neogene-Quaternary continental margin volcanism. Proceedings of the GSA Penrose Conference at Metepec, Puebla, Mexico, p 49

Parat F, Holtz F (2004) Sulfur partitioning between apatite and melt and effect of sulfur on apatite solubility at oxidizing conditions. Contrib Mineral Petrol 147:201–212

Partzsch GM, Lattard D, McCammon C (2004) Mossbauer spectroscopic determination of Fe^{3+}/Fe^{2+} in synthetic basaltic glass: a test of empirical f_{O2} equations under superliquidus and subliquidus conditions. Contrib Mineral Petrol 147:565–580

Peng G, Luhr JF, McGee JJ (1997) Factors controlling sulfur concentrations in volcanic apatite. Amer Mineral 83:1210–1224

Renne PR, Swisher CC, Deino AL, Karner DB, Owens TL, DePaolo DJ (1998) Intercalibration of standards, absolute ages, and uncertainties in $^{40}Ar/^{39}Ar$ dating. Chem Geol 145:117–152

Righter K, Rosas-Elguera J (2001) Alkaline lavas in the volcanic front of the western Mexican Volcanic Belt: geology and petrology of the Ayutla and Tapalpa volcanic fields. J Petrol 42:2333–2361

Robin C, Mossand P, Camus G, Cantagrel JM, Gourgaud A Vincent PM (1987) Eruptive history of the Colima volcanic complex (Mexico). J Volcanol Geotherm Res 31:99–113

Sack RO, Carmichael ISE, Rivers M, Ghiorso MS (1980) Ferric-ferrous equilibria in natural silicate liquids at 1 bar. Contrib Mineral Petrol 75:369–376

Samson SD Alexander EC (1987) Calibration of the interlaboratory $^{40}Ar/^{39}Ar$ dating standard, Mmhb-1. Chem Geol 66:27–34

Taylor JR (1982) An introduction to error analysis: the studies of uncertainty in physical measurements. University Science Books, Mill Valley, California, pp 1–270

Walker GPL (1973) Explosive volcanic eruptions: a new classification scheme. Geol Rund 62:431–446

Wallace PJ, Carmichael ISE (1992a) Alkaline and calc-alkaline lavas near Los Volcanes, Jalisco, Mexico: geochemical diversity and its significance in volcanic arcs. Contrib Mineral Petrol 111:423–439

Wallace PJ, Carmichael ISE (1992b) Sulfur in basaltic magmas. Geochim Cosmochim Acta 56:1863–1874

Wallace PJ, Carmichael ISE (1999) Quaternary volcanism near the Valley of Mexico: implications for subduction zone magmatism and the effects of crustal thickness variations on primitive magma compositions. Contrib Mineral Petrol 135:291–314

Westrich HR, Gerlach TM (1992) Magmatic gas source for the atmospheric SO_2 cloud from the June 15, 1991, eruption of Mount Pinatubo. Geology 20:867–870

Wood CA (1980) Morphometric analysis of cinder-cone degradation. J Volcanol Geotherm Res 8:137–160